Available online at www.sciencedirect.com

SciVerse ScienceDirect

Physics Procedia 36 (2012) 133 – 137

Physics Procedia

[a]Superconductivity Centennial Conference

Improved Characteristics of Integrated HTS rf SQUID on Bicrystal $SrTiO_3$ Substrate Resonator Covered with HTS Thin Films in Flip-Chip Geometry

Yoshimi Hatsukade*, Makoto Takemoto, Ryuichi Kurosawa, Yousuke Uchida, Saburo Tanaka

Toyohashi University of Technology, 1-1 Hibarigaoka, Tenpaku-cho, Toyohashi, Aichi 44-18580, Japan

Abstract

Integrated high-temperature superconductor (HTS) radio-frequency (rf) superconducting quantum interference devices (SQUIDs) based on a bicrystal $SrTiO_3$ substrate was investigated for application to magnetic contaminant detection. By covering a wide superconducting weak link and/or a slit of the $YBa_2Cu_3O_{7-x}$ SQUID with HTS thin films in flip-chip geometry, characteristics such as effective area and 1/f noise profile of the SQUID were successfully improved. By installing the covered SQUID in a magnetic contaminant detection system, it was demonstrated that the system can detect a tungsten ball of 15 μm in diameter with a signal to noise ratio of about 2.

PACS: 85.25.Dq; 85.25.Am,
Keywords: HTS rf SQUID; HTS thin film; flip-chip geometry; substrate resonator; bicrystal $SrTiO_3$ substrate

1. Introduction

High-temperature superconductor (HTS) radio-frequency (rf) superconducting quantum interference devices (SQUIDs) have been investigated to achieve the comparable noise performance to HTS direct-current (dc) SQUIDs [1-5]. Therefore, HTS rf SQUIDs have been widely utilized in many fields of such as nondestructive evaluation (NDE), magnetocardiogram (MCG), geophysical exploration and nuclear magnetic resonance (NMR)/magnetic resonance imaging (MRI) [6-10]. We have introduced a HTS rf

* Corresponding author.
E-mail address: hatukade@ens.tut.ac.jp

1875-3892 doi:10.1016/j.phpro.2012.06.059

SQUID with a $SrTiO_3$ (STO) substrate resonator and a flux focuser [5] into a practical magnetic contaminant detection system by taking advantage of the robustness of the SQUID [11]. For further improvement of the sensitivity of the system, we developed an integrated HTS rf SQUID on a bicrystal STO substrate resonator without a flux focuser to reduce a liftoff distance between the SQUID and room temperature. Fig. 1 shows the design of the integrated HTS rf SQUID with a rectangular hole. Based on the design, we fabricated a $YBa_2Cu_3O_{7-x}$ (YBCO) HTS rf SQUID on a bicrystal STO substrate resonator with a mis-orientation angle of 30^0. By installing the integrated SQUID into the detection system employing the SQUID microscopic technique [11, 12], we succeeded in improving the sensitivity of the system by reducing the liftoff distance to acquire a larger magnetic signal from a fine magnetic ball than that with the SQUID with the flux focuser. However, we found that the 1/f noise of the integrated SQUID (see the thin dashed line in Fig. 2) should be improved because the detection system measures magnetic signals in a low frequency range below 100 Hz from magnetized contaminants, which are moved by a belt conveyer. In this work, we investigated the characteristics of the integrated HTS rf SQUID on the bicrystal STO substrate resonator, which was covered with HTS thin films on normal STO substrates in flip-chip geometry, to improve the characteristics such as the 1/f noise and effective area. We also report the characteristics and performance of the covered SQUID, which was finally installed in the magnetic contaminant detection system.

2. Characteristics of Integrated HTS rf SQUID covered with HTS Thin Films

As shown in Fig. 1, there is a bicrystal grain boundary (GB) running across the SQUID ring to form a wide superconducting weak link, where flux trapping and moving can easily occur. There is also a slit in the left-hand of the SQUID ring, where flux focusing effect may occur. A fraction of external flux to be measured will pass through the slit. Therefore, we fabricated an YBCO thin film on a normal STO substrate, and cut it to pieces by a diamond saw to cover the wide weak link and/or the slit of the SQUID in flip-chip geometry. Thickness of the HTS thin films was about 200 nm, which is same as that of the SQUID. Area of the films was 4.1 mm x 2 mm. Positions of the HTS thin films glued on the SQUID ring with Apiezon grease are indicated by the dotted lines in Fig. 1. We pressed both the STO substrates so that the distance between the SQUID and the films became as short as possible. The film on the right-hand GB was expected to suppress flux trapping and moving in the weak link, while the film on the left-hand slit was expected to suppress the same phenomena along the edges of the slit. In addition, the latter was expected to couple external flux, which would pass through the slit without the film, to the SQUID hole due to the Meissner effect to increase the effective area of the SQUID.

The HTS rf SQUID covered with the thin films was operated by means of a commercial rf SQUID electronics to measure the characteristics such as the 1/f noise, the effective area, and the field sensitivity. The SQUID was inductively coupled with a normal conducting antenna from the electronics using the bicrystal STO substrate as a resonator. The characteristics of the SQUID with and without the HTS films were measured in a magnetically shielded room (MSR) with a shielding factor of about 60 dB while cooling the SQUID in liquid nitrogen. The resonance frequency of the electronics was about 680 MHz throughout the experiments. Each data was measured three times, and then averaged.

The experimental results were shown in Fig. 2 and summarized in Table 1. As shown in Fig. 2, the all noise profiles with the films were improved compared to that of the bare SQUID. Below 10 Hz, the best noise figure was obtained with the film on the GB only, followed by that with the film on the slit. These results indicate that the films prevented flux from trapping and moving in the wide GB and the edges along the slit. It is also suggested that the number of flux trapping and moving in the wide GB should be larger than those in the slit edges. It is unexpected that the noise in this region with the films on both the GB and the slit was higher than those in the former two cases. This may be because both the films served

to focus the existing flux during the cooling around the SQUID hole. Above 10 Hz, the latter case showed the lowest noise level with the largest effective area, followed by the case with the film on the slit. These results indicated that the film on the slit coupled the external flux, which would pass through the slit without the film, to the SQUID ring. It is noteworthy that the film on the wide GB also contributed to increase the effective area moderately. It is inferred that the possible removal of the flux trapping in the GB by the film might work to recover the superconducting area in the GB to increase the effective area.

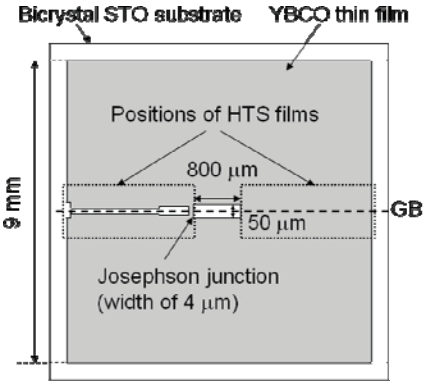

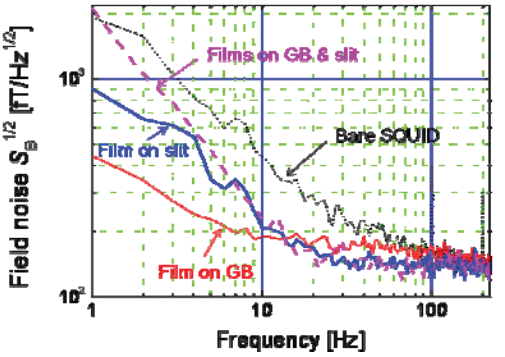

Fig. 1. Design of HTS rf SQUID based on bicrystal STO substrate. Fig. 2 Field noise profiles of SQUID with HTS films at 77 K.

Table 1. Characteristics of HTS rf SQUID with and without HTS films on GB and slit at 77 K.

SQUID conditions	A_{eff} [mm^2]	$S_B^{1/2}$ @ 1 Hz [fT/Hz$^{1/2}$]	$S_B^{1/2}$ @ 10 Hz [fT/Hz$^{1/2}$]	$S_B^{1/2}$ @ 100 Hz [fT/Hz$^{1/2}$]
Bare SQUID	0.81	1930	440	240
With film on GB	0.83	440	190	170
With film on slit	0.917	900	210	140
With films on GB and slit	0.931	2100	225	135

3. Magnetic Contaminant Detection System using HTS rf SQUID covered with HTS Films

The HTS rf SQUID covered with the HTS films on both the GB and the slit was installed in the magnetic contaminant detection system [11] utilizing the SQUID microscopic technique. The schematic figure of the SQUID mounted in the cryostat was illustrated in Fig. 3 (a). The SQUID with the films were fixed with silver past on the sapphire rod, which was connected to a copper tank filled with liquid nitrogen. In order to reduce the liftoff distance, the normal STO substrate with original thickness of 0. 5 mm was manually filed such that the thickness became to about 0.25 mm. A sapphire window with thickness of 0.5 mm separates the SQUID and the room temperature. The minimum liftoff distance between the SQUID to a sample is estimated to be about 1 mm. Fig. 3 (b) shows the noise profile of the covered SQUID installed in the system. For comparison, the noise of the bare SQUID without the films in the system is shown together. The noise level of the covered SQUID between 6 Hz to 100 Hz was lower than that of the bare SQUID. By this system, detection of fine tungsten balls with diameters of less than 100 μm was examined. In the system, a sample ball on the belt conveyer was firstly magnetized in the

vertical direction away from the SQUID, and then moved just under the SQUID at a velocity of 100 mm/s. The remnant magnetic signal from the sample ball was measured by the SQUID, and the SQUID output was recorded through a high-pass filter with a cut-off frequency of 0.5 Hz and a low-pass filter with a cut-off frequency of 20 Hz. Fig. 4 (a) shows experimental results of a tungsten ball of 100 μm in diameter measured with the bare SQUID and the covered SQUID with the liftoff distances of about 1.5 and 1.75 mm, respectively. Due to the larger effective area, the signal measured with the covered SQUID was about 10 % larger than that measured with the bare SQUID, even though the liftoff distance of the former was a bit longer than that of the latter. Fig. 4 (b) shows the relationship between diameter of the sample tungsten ball and the signal amplitude measured from the samples. As shown, the signal amplitude is approximately proportional to the cubic of the sample diameter. Since the maximum peak-to-peak noise amplitude of the system was about 0.5 pT, it is demonstrated that a tungsten ball of diameter of about 15 μm can be detectable by the system with a signal to noise ratio (S/N) of at least 2.

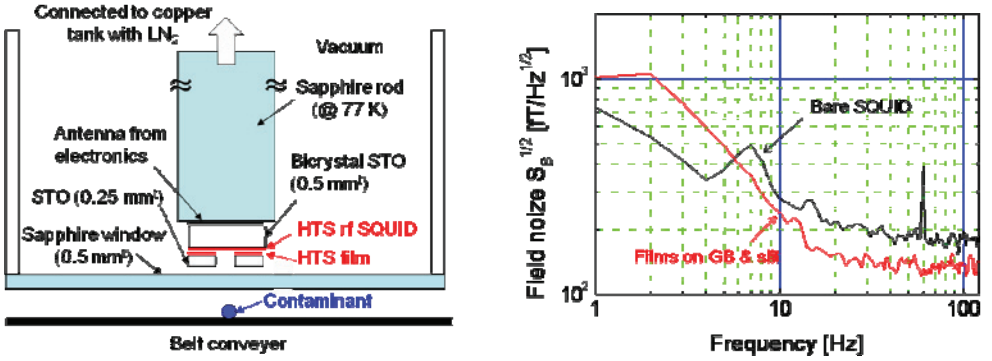

Fig. 3. (a) HTS rf SQUID with HTS films installed in microscopic cryostat; (b) Noise profile of SQUID with HTS films in cryostat.

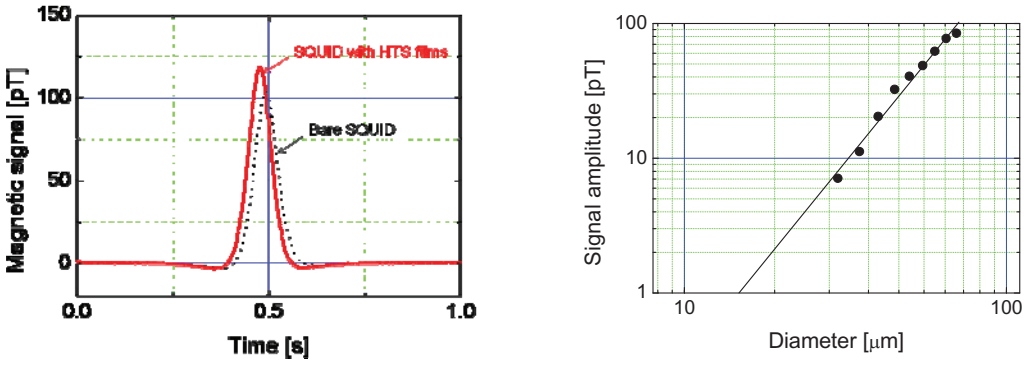

Fig. 4. (a) Magnetic signal from tungsten ball of 100 μm in diameter; (b) Signal amplitude vs. diameter of tungsten ball.

4. Conclusions

The bicrystal Josephson junction HTS rf SQUID covered with the HTS thin films in the flip-chip geometry was investigated. By covering the GB and/or the slit of the SQUID with the films, the effective area and the 1/f noise profile were successfully improved. With the two films on both the GB and the slit, the SQUID had not only the largest effective area of 0.93 mm^2, but also relatively large noise of 1 – 2 $pT/Hz^{1/2}$ at 1 Hz. By installing the covered SQUID in the magnetic contaminant detection system, it is demonstrated that the system can detect a tungsten ball of 15 μm in diameter with the S/N of at least 2.

Acknowledgements

This work is supported by “The Knowledge Hub” of Aichi, The Priority Research Project.

References

[1] Zhang Y, Muck M, Herrman K, Schubert J, Zander W, Braginski AI, Heiden C. Sensitive RF-SQUIDs and magneotmeters operating at 77K. *IEEE Trans Appl Supercond* 1993;**3**:2465-8.

[2] Ockenfuss GJ, Borgmann J, Reese M, Wordenweber R. Optimization of large-area single-layer flux-transformers and concentrators coupled to RF-SQUIDs in flip-chip geometry. *IEEE Trans Appl Supercond* 1997;7:3698-1.

[3] He DF, Zeng, XH, Krause H-J, Soltner H, Rueders F, Zhang Y. Radio frequency SQUIDs operating at 77 K with 1 GHz lumped-element tank circuit. *Appl Phys Lett* 1998;**72**:969-71.

[4] Zhang Y, Yi HR, Schubert J, Zander W, Krause H-J, Bousack H, Braginski AI. Operation of rf SQUID magnetometers with a multi-turn flux transformer integrated with a superconducting labyrinth resonator. *IEEE Trans Appl Supercond* 1999;**9**:3396-0.

[5] Zhang Y, Schubert J, Wolters N, Banzet M, Zander W, Krause H-J. Substrate resonator for HTS rf SQUID operation. *Physica C* 2002;**372-376**:282-6.

[6] Hohmann R, Maus M, Lomparski D, Gruneklee M, Zhang Y, Krause H-J, Bousack H, Braginski AI. Aircraft wheel testing with machine-cooled HTS SQUID gradiometer system. *IEEE Trans Appl Supercond* 1999;**9**:3801-4.

[7] Kreutzbruck MV, Baby U, Theiss A, Mueck M, Heiden C. Inspection of aircraft parts with high remnant magnetization by eddy current SQUID NDE. *IEEE Trans Appl Supercond* 1999;**9**:3805-8.

[8] Zhang Y, Panaitov G, Wang SG, Wolters N, Otto R, Schubert J, Zander W, Krause H-J, Soltner H, Bousack H, Braginski AI. Second-order, high-temperature superconducting gradiometer for magnetocardiography in unshielded environment. *Appl Phys Lett* 2000;**76**:906-8.

[9] Foley CP, Leslie KE, Bink R, Lewis C, Murray W, Sloggett GJ, Lam S, Sankrithyan B, Savvides N, Katzaros A, Muller K-H, Mitchell EE, Pollock J, Lee J, Barrow DL, Asten M, Maddever A, Panjkovic G, Downey M, Hoffman C, Turner R. Field trials using HTS SQUID magnetometers for ground-based and airborne geophysical applications. *IEEE Trans Appl Supercond* 1999;**9**:3786-92.

[10] Fukumoto S, Hayashi M, Katsu Y, Hatsukade Y, Tanaka S, Snigirev O. Liquid-state nuclear magnetic resonance measurements for imaging using HTS-RF-SQUID in ultra-low field. *IEEE Trans Appl Supercond* 2011;**21**:522-5.

[11] Takemoto M, Akai T, Kitamura Y, Hatsukade Y, Tanaka S. HTS-RF-SQUID microscope for metallic contaminant detection. *IEEE Trans Appl Supercond* 2011;**21**: 432-5.

[12] Chen J-C, Chen K-L, Yang H-C, Wu C-H, Horng H-E. Integrated high-T_c radio frequency superconducting quantum interference device using $SrTiO_3$ bicrystal substrate resonators. *Appl Phys Lett* 2007;**90**:153504-6.